

## THERMAL ANALYSIS OF A JET IMPINGING AGAINST A PLATE WITH AND WITHOUT A POROUS LAYER

Cleves Fischer, cleves@ita.br

Marcelo J.S. de Lemos, delemos@ita.br

Departamento de Energia - IEME

Instituto Tecnológico de Aeronáutica - ITA

12228-900 - São José dos Campos - SP - Brasil

**Abstract.** *Impinging jets are widely used in industrial processes as an efficient mechanism of heating or cooling of the surfaces. In incidence region of the jet, has increase of the local Nusselt number and, depending of the distance between jet and surface, a second peak of this parameter is observed. These variations in the distribution of the local Nusselt number can be desired or not, depending on the specific application considered. The use of porous medium between the surface and the jet can to allow a control of the local heat exchange. Inspired by this, this work shows numerical results for a jet impinging against a flat plane with and without porous layer. Parameters such as porosity and thickness of the porous layer are varied in order to analyze their effects on the ditribution of the local Nusselt number. The macroscopic time-average equations for mass, momentum and energy are obtained based on the Double Decomposition concept (spatial deviations and temporal fluctuations).The numerical technique employed for discretizing the governing equations is the control volume method with a boundary-fitted non-orthogonal coordinate system. The SIMPLE algorithm is used to handle the pressure-velocity coupling. For numerical solution, a structured computational grid is used, refined at the incidence region.*

**Keywords:** *Porous Media, Impinging Jet, Nusselt Number, Numerical Simulation*

### 1. INTRODUCTION

Impinging jets are widely used in industrials applications in order to heat, cool or drying surfaces. These applications include electronics components cooling, glass tempering, annealing of metals, drying of textiles products and papers. The main advantage of impinging jets is its ability to produces high localized mass and heat transfer rates due to the thin layer, hydrodynamics and thermal, inside of the stagnation flow region.

The literature studies are mainly concentrate in the impinging jets analysis with high Reynolds number. The pioneer studies, considering two-dimensional impinging jets with low Reynolds number, have been conducted by Gardon and Akfirat (1966) that have get experimentally the local and average coefficients of heat transfer for this flow. Sparrow and Wong (1975) obtained experimentally the distribution coefficients of local mass transfer for a two-dimensional impinging jet, being the results converted to heat transfer through the analogy between mass and heat transfer. Chen *et al.* (2000) experimentally and numerically analyzed the mass and heat transfer induced for a two-dimensional laminar jet. Chiriac and Ortega (2002) numerically analyzed the hydrodynamic and heat transfer behavior in permanent and transitory regime, for a two-dimensional jet impinging against a plate with constant temperature.

The porous medium study is relatively recent, and currently it is being explored in many technological applications. But, the use of porous medium under impinging jets is little explored in the literature. Some examples are the works of Prakash *et al* (2001a) that obtained a flow visualization of turbulent jets impinging against a porous medium, Fu and Wong (1997) that evaluated the thermal performance of different porous layers under a impinging jet and Jeng and Tzeng (2005) that studied the hydrodynamic and thermal performance of a jet impinging on a metallic foam.

Analyze of thermal effects for a laminar impinging jet with the presence of a porous medium have not been studied. Motivated by foregoing, this work intends to investigate the laminar, confined and two-dimensional impinging jet, acting on a flat plate with or without a covering of a porous layer. The flow in porous medium modeling used in this paper is based on the Pedras and de Lemos (2000) work that developed a macroscopic model of two equations. The work of Rocamora and de Lemos (2000) adds thermal modeling for a medium with a porous matrix. In addition to the model was incorporated the work of Silva and de Lemos (2001) that presented numerical solutions for laminar and turbulent flows in a hybrid medium considering the shear stress jump at the interface between porous and clear medium.

### 2. PROBLEM DESCRIPTION

The geometries and nomenclature of the problem are presented in Fig. 1. A laminar jet with uniform or fully developed velocity profile  $v_o$  and at a constant temperature  $T_o$  enters from a nozzle into a channel with height  $H$  and length  $2L$  shaped for two flat parallel plates. The jet impinges normally against the inferior channel plate characterizing a two-dimensional and confined impinging jet. The width of nozzle is  $B$  and the nozzle-to-plate spacing is  $H$ . The

inferior plate temperature  $T_1$  is maintained constant and 10K above the temperature of entering jet  $T_o$ . The inferior plate can be covered by a porous layer of height  $h$ .

The flow is assumed two-dimensional, laminar, incompressible and unsteady. The porous medium is assumed homogeneous, rigid and inert. The properties of the fluid are constant and gravity effects are not considered.

The boundary conditions of the problem are: constant or fully developed velocity profile and constant temperature profile of the entering jet; no slip condition in the walls; symmetry condition in  $x = 0$ ; velocity and temperature profile fully developed in channel exit ( $x = L$ ); at the inferior plate ( $y = H$ ) constant temperature condition is assumed; at the superior plate, for  $B/2 < x \leq L$ , null heat flux condition is assumed.

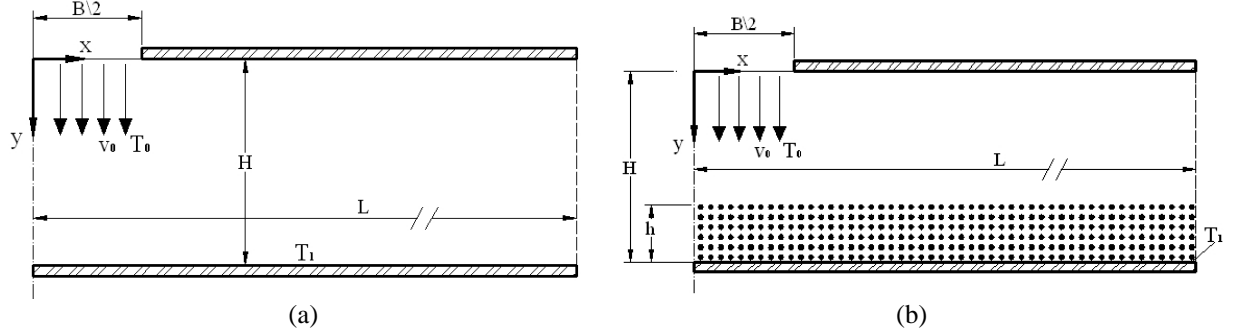


Figure 1 - Analyzed geometries (a) clean medium (b) porous medium

### 3. MATHEMATICAL MODELING

For numerical flows resolution in porous medium, a series of pertinent concepts to the problem such as intrinsic volumetric average, spatial deviation, local volumetric average theorem, the macroscopic conservation equations and the double decomposition concept are used as they have been presented in the works of Pedras and de Lemos (2000) and Pedras and de Lemos (2000b).

For the porous medium flow, the general formulation for continuity and momentum macroscopic equations are given by:

$$\nabla \cdot \mathbf{u}_D = 0 \quad (1)$$

$$\rho \nabla \cdot \frac{\mathbf{u}_D \mathbf{u}_D}{\phi} = -\nabla \phi \langle p \rangle^i + \mu \nabla^2 \mathbf{u}_D - \left[ \frac{\mu \phi}{K} \mathbf{u}_D + \frac{c_f \phi \rho}{\sqrt{K}} |\mathbf{u}_D| \mathbf{u}_D \right] \quad (2)$$

These equations are valid for both clean and porous medium, where  $\langle p \rangle^i$  is the intrinsic pressure average in the fluid,  $u_D$  is the average surface velocity or Darcy velocity,  $x$  and  $y$  are the Cartesian coordinates,  $\mu$  is the fluid viscosity,  $\phi$  is the porous medium porosity and  $K$  is the porous medium permeability. The Eq. (1) is the mass conservation equation and Eq. (2) represents the momentum conservation. The third and fourth terms on the right hand side of Eq. (2) are the Darcy's and Forchheimer's terms, respectively.

The macroscopic energy equation for laminar flow in porous medium, using the local thermal equilibrium hypothesis, is fully detailed in the work of Rocamora and de Lemos (2000), and is given by:

$$(\rho c_p)_f \nabla \cdot \left( \phi \langle \mathbf{u} T \rangle^i \right) = (\rho c_p)_f \nabla \cdot \left\{ \phi \left( \langle \mathbf{u} \rangle^i \langle T_f \rangle^i + \langle \mathbf{u}^i T_f \rangle^i \right) \right\} \quad (3)$$

where,  $c_p$  is the fluid specific heat,  $T_f$  is the fluid temperature and  $\mathbf{u}$  is the flow velocity. To the last two terms on the right hand side of Eq. (3) could be given the following physical significance: penultimate term is the convective heat flux based on macroscopic time mean velocity and temperature; last term is thermal dispersion associated with deviations of microscopic time mean velocity and temperature.

The above equations are simplified for clean medium particular equations when  $\phi$  is 1 and  $K$  tending to infinite.

#### 4. NUMERICAL METHOD

Equations (1), (2) and (3) subject to interface and boundary conditions were discretized in a two-dimensional control volume involving both clear and porous mediums. The equations discretization uses a system of generalized coordinates. The finite volumes method was used in the discretization and the SIMPLE algorithm (Patankar,1980) was used to the treatment of pressure-velocity coupling.

The Fig. 2 present a typical control volume together with the generalized coordinates system,  $\eta - \xi$ . The general and discretized form of the two-dimensional conservation equation of a generic property  $\varphi$ , in permanent regime, is given by:

$$I_e + I_w + I_n + I_s = S_\varphi \quad (4)$$

where  $I_e$ ,  $I_w$ ,  $I_n$  and  $I_s$  represent, respectively, the fluxes of  $\varphi$  in the faces east, west, north and south of the control volume and  $S_\varphi$  its term source.

Every time the source term is dependent of  $\langle \varphi \rangle^i$ , it will be linearized in the following form:

$$S_\varphi \approx S_\varphi^{**} \langle \varphi \rangle_P^i + S_\varphi^* \quad (5)$$

The source terms in the momentum equations to  $x$  direction are given by:

$$S^{*x} = (S_e^{*x})_P - (S_w^{*x})_P + (S_n^{*x})_P - (S_s^{*x})_P + S_P^* \quad (6)$$

$$S^{**x} = S_\phi^{**} \quad (7)$$

where,  $S^{*x}$  is the diffusive part treated in explicit form. The term  $S^{**x}$  in the equation for the porous medium is composed by the term of Darcy coefficient in the  $x$  direction.

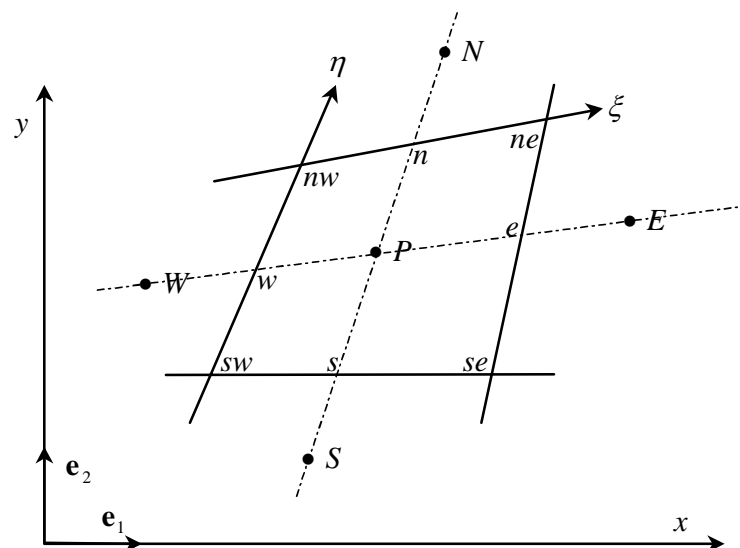


Figure 2 – Control volume and notation

#### 5. RESULTS AND DISCUSSION

In all numerical simulations were used a 40 x 150 (6000 nodes) grid, refined next to the walls. The grid and computational code validation for clean medium are made comparing the obtained results with literature data for two different configurations.

Figure 3a shows the distribution of the local Nusselt number close to the incidence inferior plate and it is compared with experimental data of Gardon and Akfirat (1966) and numerical results of Chen *et al.* (2000). In order to make the comparison it is necessary to normalize the local Nusselt with  $Pr^{-1/3}$ . The Reynolds number is  $Re = 450$ , the inlet

velocity profile is fully developed for a flow between parallel plates (Fox, 1998), the temperature profile is uniform and the ratio between the nozzle-to-plate spacing and nozzle width is  $H/B = 4$ .

Figure 3b shows the comparison of local Nusselt number close to inferior plate with the numerical results of Chiriac and Ortega (2002). The inlet velocity and temperature profiles are uniform and the ratio between the nozzle-to-plate spacing and nozzle width is  $H/B = 5$ .

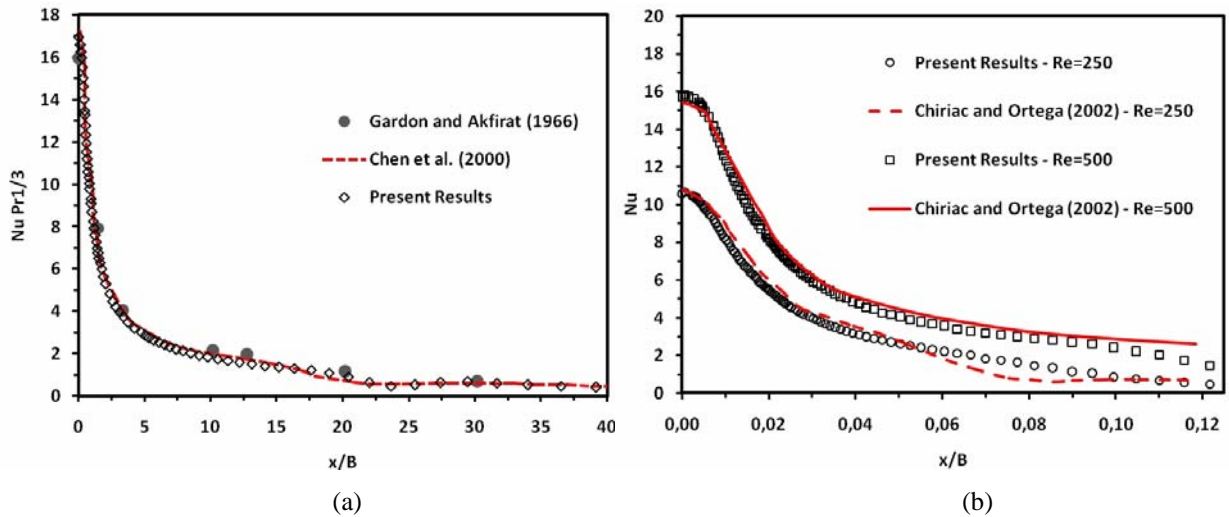


Figure 3 - Distribution of  $Nu$  on the inferior plate for clean medium. (a)  $H/B = 4$  (b)  $H/B = 5$

The Fig. 3 shows that results have very good accordance with values found in the literature, confirming the code and used grids validation.

Do not have comparative data in the literature for this problem in porous medium, so its validation is impossible.

The impinging jets flow presents three distinct characteristics regions (Incropera, 2003). The entrance region is termed the *free jet*, in this region the flow conditions are unaffected by the impingement (target) surface and the jet axial velocity is almost constant to its nominal value. The *stagnation region* corresponds to the region where the flow is influenced by the impingement surface, it is decelerated and almost all kinetic energy is transformed into a static pressure rise. Following impact the jet flow is redirected and accelerated again along the target surface. However the horizontal accelerated flow cannot continue indefinitely accelerating and it is transformed on a decelerating *wall jet*, comprising the boundary layer. The above characteristics of the flow in stagnation region come out on peaks of the Nusselt number as show Fig. 3.

All the following results have been simulated with the following geometric configurations and boundary conditions: uniform velocity and temperature profile; inlet jet temperature  $T_1 = 300K$ ; the inferior plate temperature is maintained constant and equal to  $T_o = 300K$ ; the ratio between the nozzle-to-plate spacing and nozzle width is maintained constant and equal to  $H/B = 2$ ; the nozzle width is  $B = 1 \times 10^{-03} m$ .

Figures 4 and 5 respectively, show the streamlines and temperature field for various Reynolds numbers and for the inferior plate without porous cover.

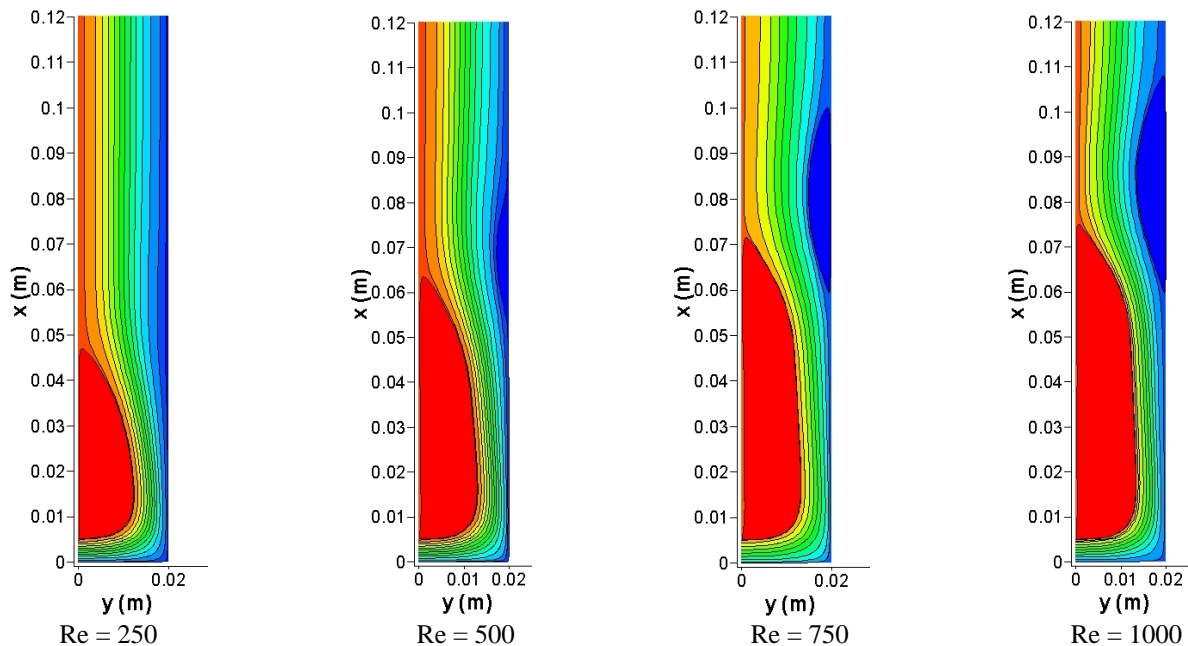


Figure 4 - Streamlines for clean medium and  $H/B = 2$  for various Reynolds numbers

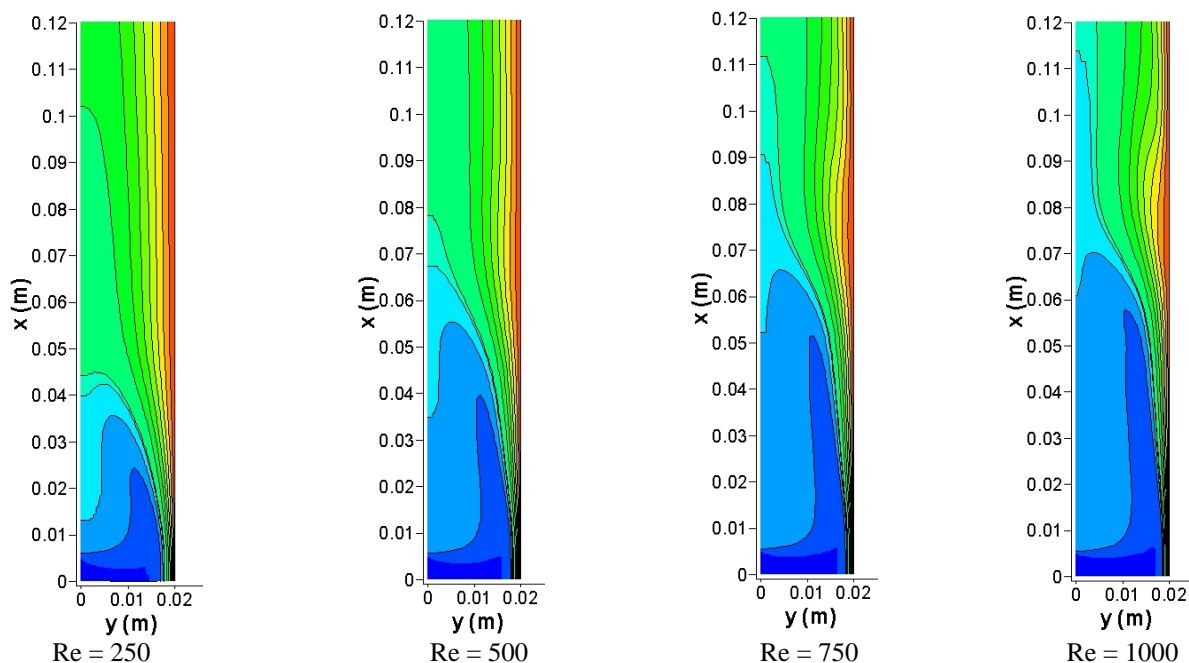


Figure 5 – Temperature distribution fields for clean medium and  $H/B = 2$  for various Reynolds numbers

In Fig. 4 it can be seen a primary recirculation near the inlet jet region, it is mainly due to the mixture of the outlet nozzle flow with fluid in the rest medium. In addition, when the Reynolds number increases, a secondary region of recirculation appears close to the inferior wall plate. In Fig. 5 it is observed that, as expected, the temperature fields suffer deformation in the regions where the recirculation appears. Also, it is verified that the isothermals are very close to target plate in the stagnation flow region.

For a performance analysis of heat transfer due to the jet velocity variation, the Fig. 6 shows a graph with the local Nusselt number close to the target plate for various Reynolds numbers.

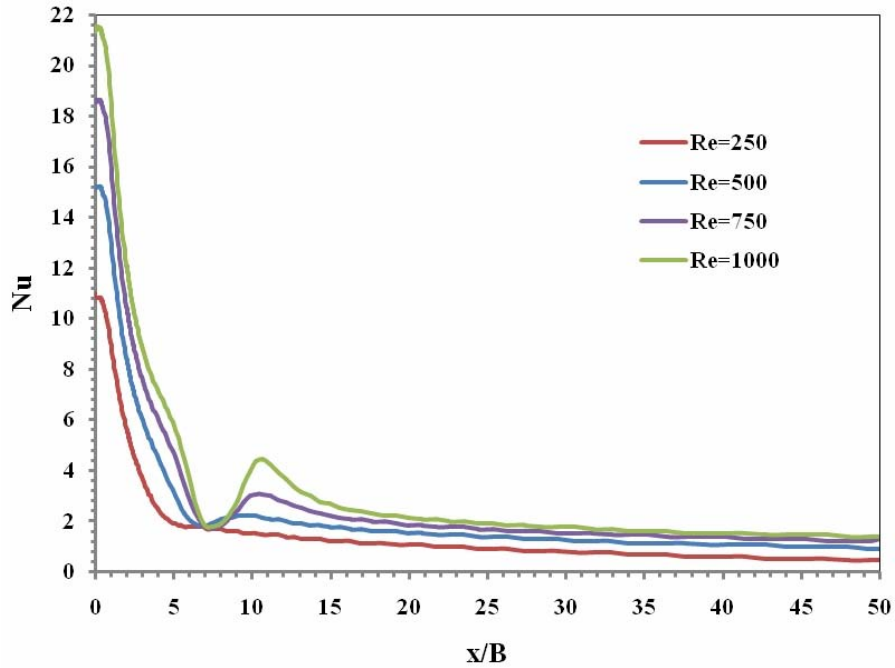


Figure 6 – Local Nusselt distribution close to the inferior plate for clean medium and  $H/B = 2$  .

As the Reynolds number increases, the Nusselt number peak in the stagnation region ( $x = 0$ ) increases, as show in Fig. 6. In addition, it can be seen that appear a second Nusselt peak for Reynolds number greater than  $Re = 500$  and about for  $x/B = 10$  . This second peak is connected to the recirculation region showed in Fig. 4, and it can be attributed to the engulfing motion around the secondary recirculation region which reduces the thickness of the thermal boundary layer (Chung and Luo (2002)).

Figures 7 and 8 show the streamlines and temperature fields for a configuration with the insertion of a porous layer of thickness  $h = 0.5H$  covering the inferior plate. The Reynolds number is maintained constant and equal to  $Re = 750$  .

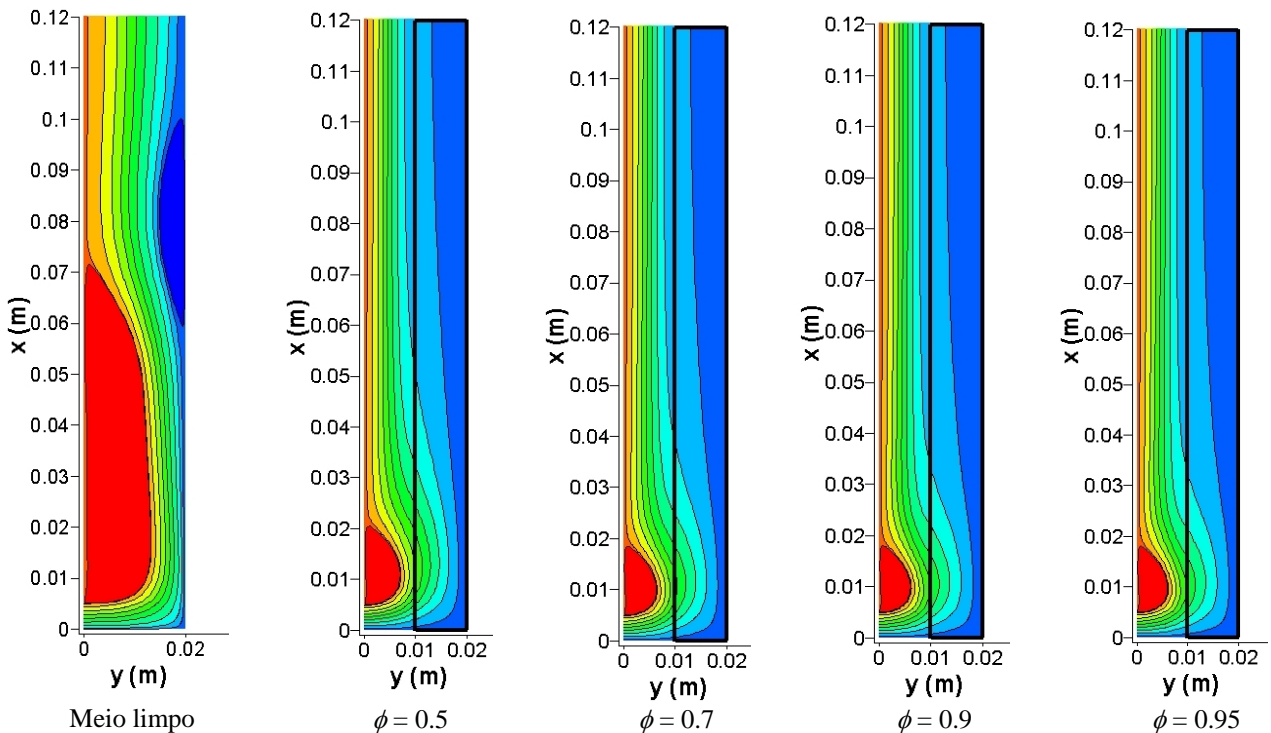


Figure 7 - Streamlines for various porosities with  $Re = 750$  ,  $H/B = 2$  and  $h = 0.5H$  .

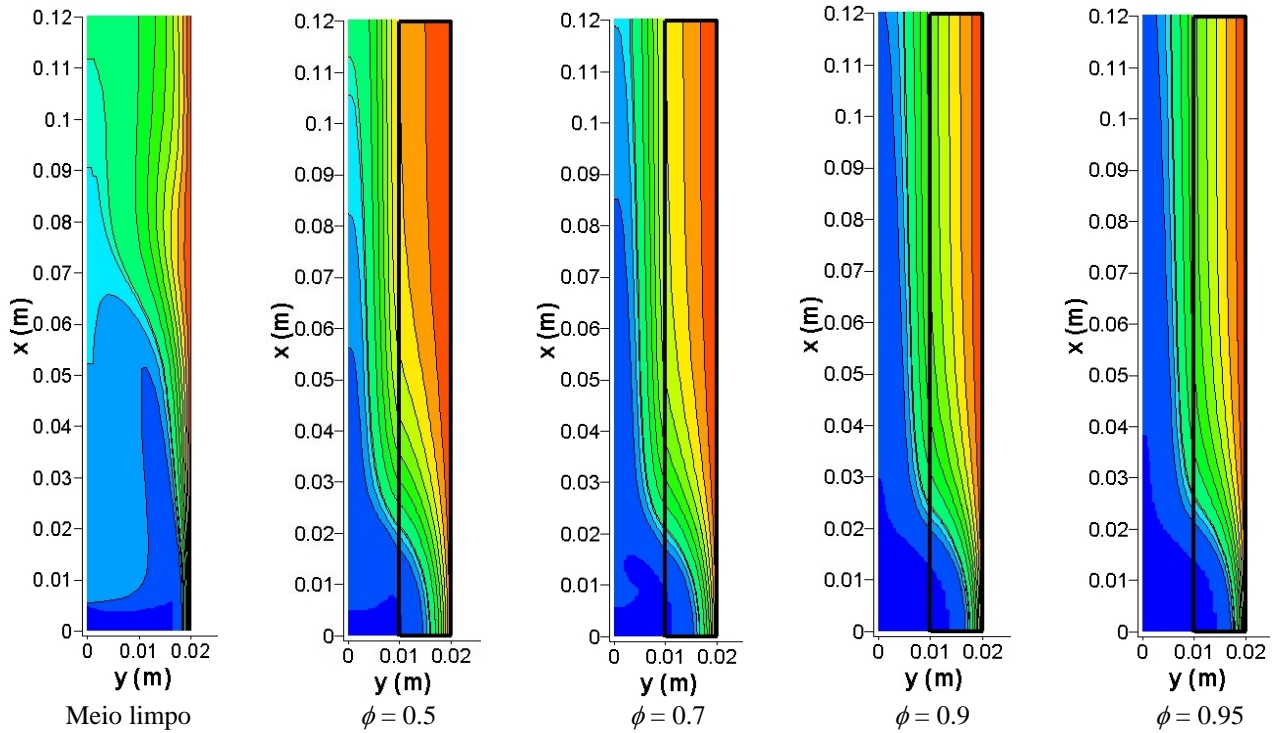


Figure 8 – Temperature fields for various porosities with  $Re = 750$ ,  $H/B = 2$  and  $h = 0.5H$ .

The Fig. 7 shows that the porosity variation do not strongly influences the flow behavior, it is confirmed in the work of Graminho and de Lemos (2004). On the other hand, in Fig. 8 it is possible to perceive that as porosity increases the field temperature becomes more quickly homogeneous. Also, for porosity increases the isothermal lines in the stagnation region becomes more close to the inferior wall, indicating a possible greater heat exchange.

To analyze the porosity influence in the heat transfer it is presented in Fig. 9 the distribution of local Nusselt number. Again, the configuration has the insertion of a porous layer of thickness  $h = 0.5H$  and the Reynolds number is maintained constant and equal to  $Re = 750$ .

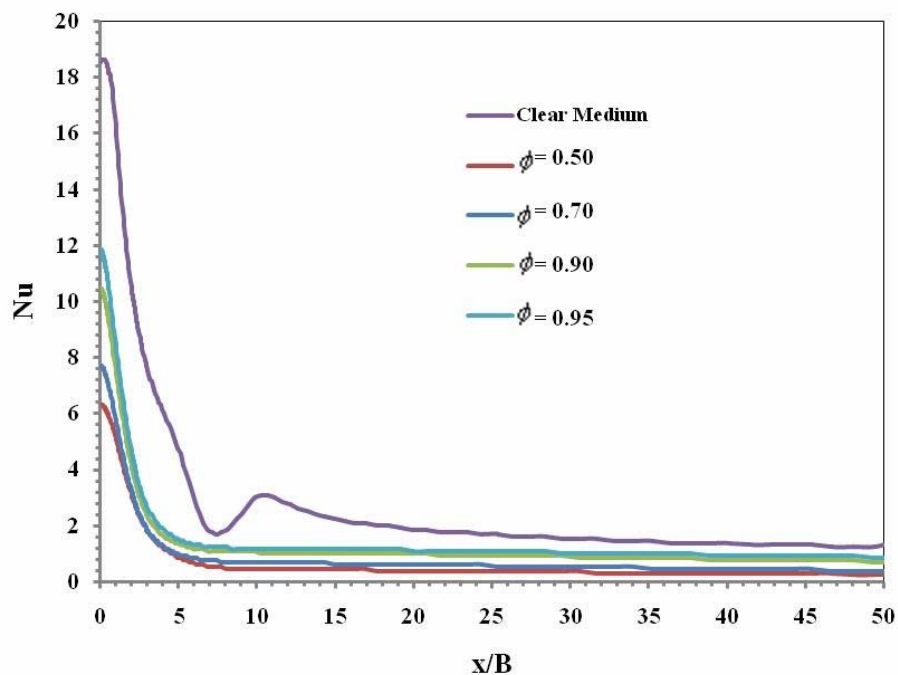


Figure 9 - Local Nusselt distribution for various porosities with  $Re = 750$ ,  $H/B = 2$  and  $h = 0.5H$ .



The insertion of a porous layer eliminates the second peak of Nusselt number, and the curve of Nusselt distribution is characterized by a peak in the stagnation region and away from the stagnation region it decreases to a minimum constant value as show in Fig. 9. In addition, porosity increases implies on the increases in stagnation Nusselt number. Then with the insertion of a porous layer the distribution of Nusselt number becomes more homogeneous and it can allow a control of the heat transfer coefficients.

Finally a study of the influence of the porous layer thickness in the heat transfer is presented. The streamlines and the field temperature for a simulation with various porous layer thicknesses, with  $Re = 750$ ,  $H/B = 2$  and  $\phi = 0.90$  are presented in Fig. 10 and 11, respectively.

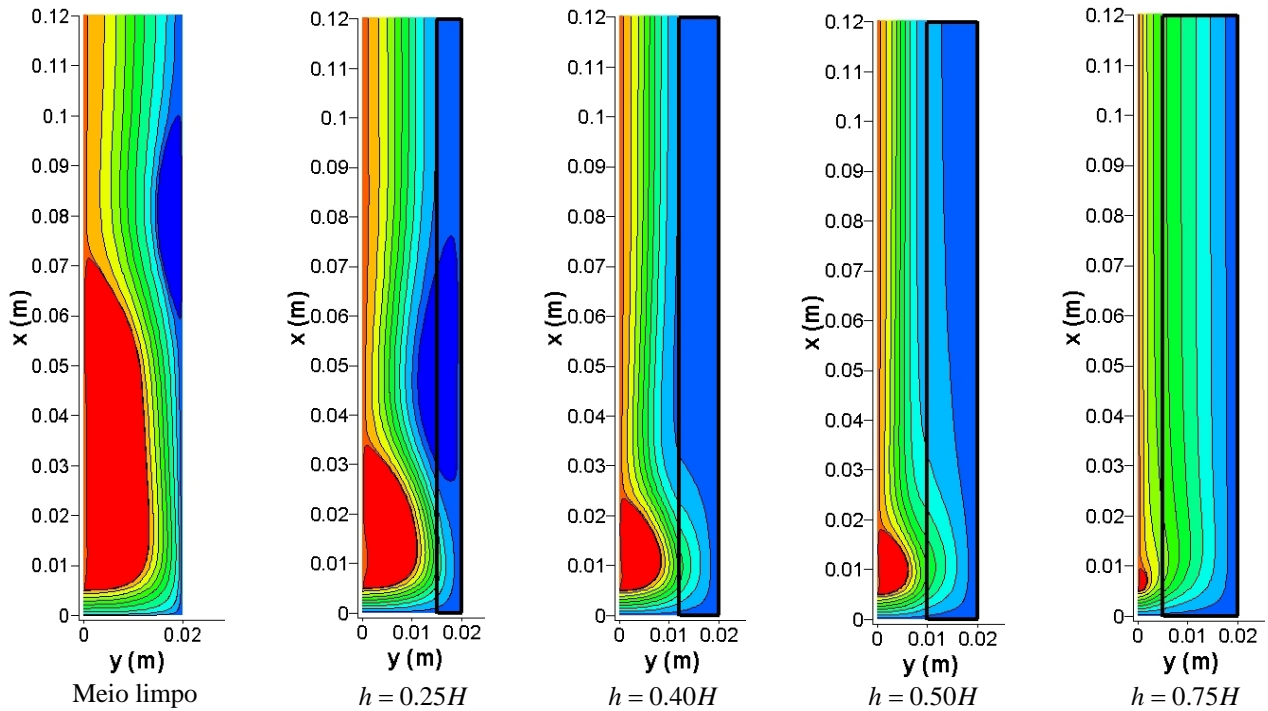


Figure 10 – Streamlines for various porous layer thicknesses with  $Re = 750$ ,  $H/B = 2$  and  $\phi = 0.9$

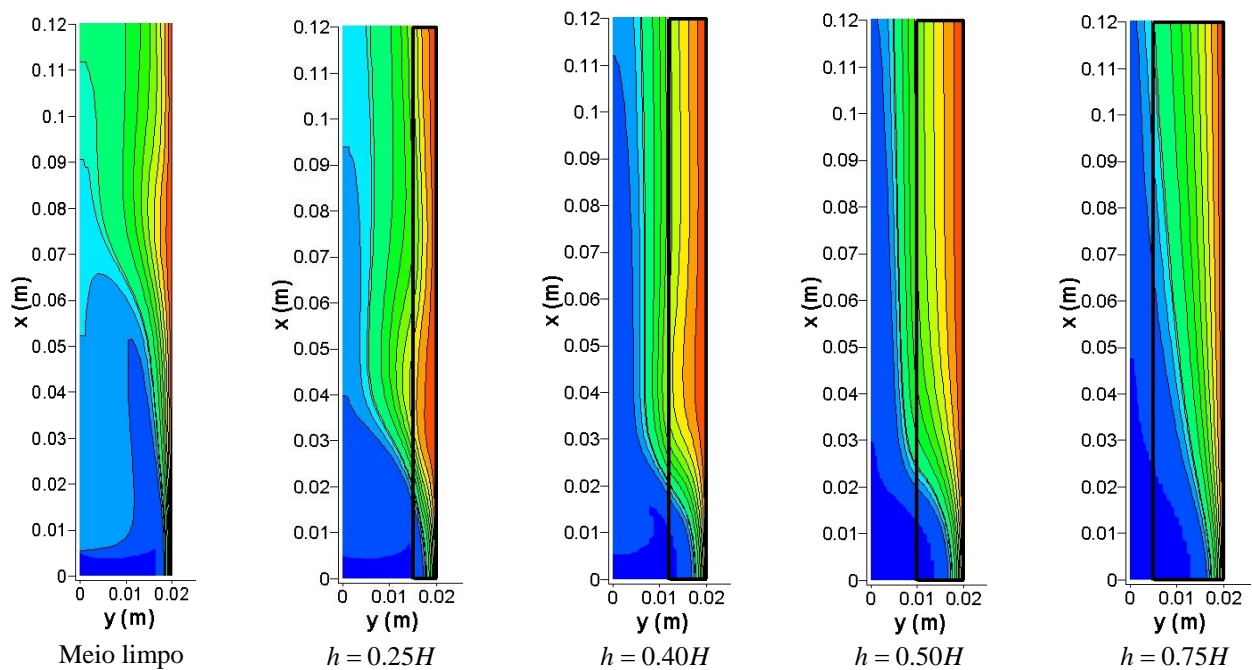


Figure 11 – Temperature fields for various porous layer thicknesses with  $Re = 750$ ,  $H/B = 2$  and  $\phi = 0.9$



Figure 10 shows that porous layer thickness strongly influences the flow behavior. For  $h = 0.25H$  the primary vortex diminishes and the second vortex has its size increased. But increasing  $h$  from  $h = 0.25H$ , the secondary vortex disappears and the primary diminishes its size. The temperature field also is influenced by the porous layer thickness variation as shows in Fig. 11. To thickness until  $h = 0.50H$  the direction of the isothermals varies more strongly mainly in the stagnation region, but it does not to happen for the thickness  $h = 0.75H$  where the isothermals lightly varies throughout the temperature field.

To complete the analysis is presented in Fig. 12 the local Nusselt number for various thickness of porous layer.

The stagnation Nusselt peak diminishes with the insertion of the porous layer, and for thicknesses inferior to  $h = 0.40H$  the second Nusselt peak continues present as shows Fig. 12. The presence of the second Nusselt peak is connected with the secondary vortices that appear in Fig. 10. Also can be seen that the variation of thickness of porous layer do not influences the value of stagnation Nusselt peak as strongly as the variation of porosity of the porous layer as can be compared by Fig. 9 and 12. The main influence of thickness of the porous layer is the change in format of the Nusselt distribution curve, once the Nusselt peak value and the minimum constant Nusselt value are similar for all thickness.

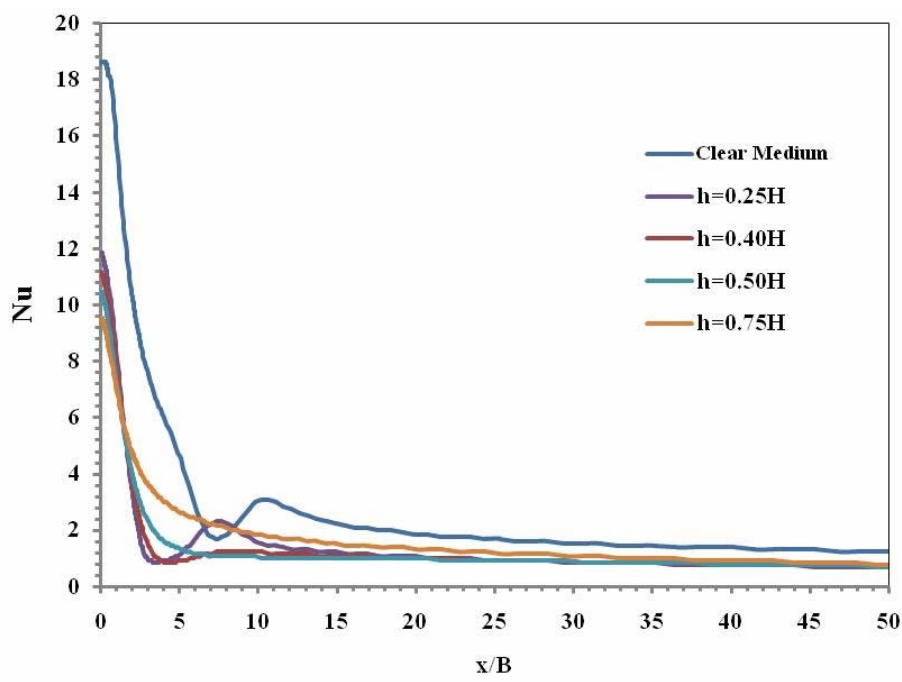


Figure 12 - Local Nusselt distribution for various porous layer thicknesses with  $Re = 750$ ,  $H/B = 2$  and  $\phi = 0.9$

## 6. CONCLUSIONS

The presence of a porous layer on the plate of the jet incidence can eliminates the second Nusselt number peak and allows controlling the heat transfer condition. It were observed that the porosity variation strongly influences the stagnation Nusselt value, while the porous layer thickness influences more strongly the format of Nusselt number distribution curve.

The purpose of this paper is contributed at engineering applications that use impinging jets how heat transfer mechanism, making available results for it. In future works the purpose is to evaluate other parameters as permeability and distance between the confinement plates, aiming to obtain situation with different characteristic of heat transfer.

## 7. ACKNOWLEDGEMENTS

The authors are thankful to FAPESP for their financial support during the preparation of this work

## 8. RESPONSIBILITY NOTICE

The authors are the only responsible for the printed material included in this paper.

## 9. REFERENCES

- Chen, M., Chalupa, R., West, A.C. and Modi, V., 2000, "High Schmidt Mass Transfer in a Laminar Impinging Slot Jet", *International Journal of Heat and Mass Transfer*, Vol.43, pp. 3907-3915.
- Chiriac, V.A. and Ortega, A., 2002, "A Numerical Study of the Unsteady Flow and Heat Transfer in a Transitional Confined Slot Jet Impinging on an Isothermal Surface", *International Journal of Heat and Mass Transfer*, Vol.45, pp. 1237-1248.
- Chung, M.Y., Luo, K.H., 2002, "Unsteady Heat Transfer Analysis of an Impinging Jet", *Journal of Heat Transfer*, Vol. 124, pp. 1039-1048.
- De Lemos, M.J.S. and Pedras, M.H.J., 2000a, "Simulation of Turbulent Flow Through Hybrid Porous Medium-Clear Fluid Domains", *Proc. of IMECE2000-ASME-Intern. Mech. Eng. Congr.*, ASME-HTD-366-5, pp. 113-122, ISBN: 0-7918-1980-6, Orlando, Florida, November 5-10.
- De Lemos, M.J.S. and Pedras, M.H.J., 2000b, "Modeling Turbulence Phenomena in Incompressible Flow Through Saturated Porous Media", *Proc. of 34th ASME-National Transfer Conference (on CD-ROM)*, ASME-HTD-I463CD, Paper NHTC2000-12120, ISBN: 0-7918-1997-3, Pittsburgh, Pennsylvania, August 20-22.
- De Lemos, M.J.S. and Pedras, M.H.J., 2001, "Recent Mathematical Models For Turbulent Flow In Saturated Rigid Porous Media", *Journal of Fluids Engineering*, vol. 123, n°4.
- Fox, R.W., McDonald, A.T., "Introdução à Mecânica dos Fluidos", 4ª edição, editora LTC, 1998.
- Fu, W.-S. and Huang, H.-C., 1997, "Thermal performance of different shape porous blocks under an impinging jet", *International Journal of Heat and Mass Transfer*, Vol. 40, No. 10, pp. 2261-2272.
- Gardon, R. and Akfirat, J.C., 1966, "Heat Transfer Characteristics of Impinging Two-Dimensional Air Jets", *Journal of Heat Transfer*, Vol.101, pp. 101-108.
- Graminho, D.R., De Lemos, M.J.S., 2004, "Características fluidodinâmicas de jatos impingentes laminares atuando sobre uma placa plana coberta com camada porosa" (em CD-ROM) ENCIT2004, Rio de Janeiro-RJ
- Incropera, F.P., De Witt, D.P., "Transferência de Calor e de Massa", 5ª edição, editora LTC, 2003.
- Jeng, T.-Z. and Tzeng, S.-C., 2005, "Numerical Study of Confined Slot Jet Impinging on Porous Metallic Foam Heat Sink", *International Journal of Heat and Mass Transfer*, Vol.48, pp. 4685-4694.
- Patankar, S.V., 1980, "Numerical Heat Transfer and Fluid Flow", Hemisphere, New York.
- Prakash, M., Turan, F.O., Li, Y., Manhone, J. and Thorpe, G.R., 2001, Impinging Round Jet Studies In A Cylindrical Enclosure With And Without A Porous Layer: Part I: Flow Visualizations And Simulations, *Chemical Engrg Science*, Vol.56, pp. 3855-3878
- Prakash, M., Turan, F.O., Li, Y., Manhone, J. and Thorpe, G.R., 2001, Impinging Round Jet Studies In A Cylindrical Enclosure With And Without A Porous Layer: Part II: DLV Measurements And Simulations, *Chemical Engrg Science*, Vol.56, pp. 3879-3892
- Rocamora, Jr. F.D. and de Lemos M.J.S., 2000, "Analysis of Convective Heat Transfer for Turbulent Flow in Saturated Porous Media", *International Communication of Heat and Mass Transfer*, Vol.27, No.6, pp. 825-834.
- Sparrow, E.M. and Wong T.C., 1975, "Impinging Transfer Coefficients due to Initially Laminar Slot Jets", *International Journal of Heat and Mass Transfer*, Vol.18, pp. 597-605.
- Silva, R.A., de Lemos, M.J.S., 2001a, "Escoamento Laminar em um Canal Parcialmente Preenchido com Material Poroso", (em CD-ROM) COBEM2001, Uberlândia-MG.